Supplemental Methods

Caerulein treatment

Acute pancreatitis was induced in p48Cre, p48Cre;Numb$^{f/f}$, p48Cre;Kras^{G12D} and p48Cre;Kras^{G12D};Numb$^{f/f}$ mice at 5-6 weeks after birth with a typical weight range of 22-25g by caerulein injection as previously described [13]. Briefly, mice received 8 hourly i.p caerulein injections (American Peptide Company), 2ug/injection on 2 consecutive days. Day 0 is counted as immediately following the final injection.

Immunohistochemistry and immunofluorescence

For histological, immunohistolochemical and immunofluorescence analysis, dissected pancreata were fixed with zinc buffered formalin (Anatech) overnight and embedded in paraffin wax. Heat mediated antigen retrieval was performed with Citra antigen retrieval solution (BioGenex) prior to staining. For immunofluorescence, AlexaFluor tagged secondary antibodies (1:400, Invitrogen) were used and slides were mounted using DAPI-containing Vectashield media (Vector). For Amylase, CK19 and CD45 immunohistochemistry, biotinylated goat anti-rat secondary (1:400, Vector) was used. 3-3'-Diaminobenzidine tetrahydrochloride was used as a chromagen. Sections were countedstained with Meyer's Hematoxylin and 1% Alcian Blue 8GX (Sigma) in 3% acetic acid solution where indicated. Primary antibodies used may be found in Supplementary Table 1.

Fluorescent images were acquired using Zeiss AxioImager and Leica SP5 confocal microscopes. Brightfield images were acquired using a Zeiss Axio Imager D1 microscope.

Western blotting

Primary antibodies are listed in Table S1. Secondary antibodies used were goat anti-rabbit IR800 and goat anti-mouse IR680 (1:15,000, LI-COR). Imaging was performed on a LI-COR Odyssey scanner and quantification was performed by normalizing fluorescence intensity of each individual band to the corresponding intensity of GAPDH.

Flow cytometry

FACS enrichment of acinar and ductal cells was performed as described by Morris et al (in preparation). Pancreata were digested with a series of reagents: 1) 2.5mg/ml Collagenase D (Roche) with 0.1ng/ml DNase I (Sigma-Aldrich) in Hank's buffered saline solution, 2) 0.05% Trypsin-EDTA, 3) 2U/ml Dispase (Invitrogen) in HBSS. Single cells were stained with FITC-conjugated anti-CD45 (1:400, eBioscience), PE-conjugated anti-CD49f (1:50, eBioscience) and Biotin-conjugated CD133 (Prominin1, 1:50, eBioscience). APC-conjugated streptavidin (1:100, eBioscience) was used as a secondary antibody. Cells were isolated using a FACS Aria (BD BioScience).

Quantification

For quantification of duct structures with luminal cells, percent metaplastic area and Alcian blue postive lesion count, 5-10 non-overlapping 100x (for p48Cre samples) or 200x (for $p48Cre^{ER}$;$Kras^{G12D}$ samples) H&E images were taken per

sample and scored by hand. Metaplastic area, in pixels, was selected by hand in Adobe Photoshop, Alcian blue positive lesions and duct structures with luminal cells were counted by hand and normalized to total area in pixels calculated by Metamorph. For Insulin/CPA1 area tissue sections from paraffin embedded pancreata were collected every 100μm through the entire organ. Sections were stained for Insulin and Cpa1 and total positive areas of each marker were calculated using a GE InCell Imager system.

Statistical Analysis

Results are shown as the mean ±SD. Paired data were evaluated using a two-tailed Student's *t*-test. Luminal cell count data was evaluated by Chi squared test. For meta-analysis of Numb expression in human PDA, 3 independent datasets[36-38] were utilized from the Oncomine microarray database (Compendia Bioscience, Ann Arbor, MI). Each study was evaluated independently using a two-tailed Student's *t*-test and a combined p value was calculated using Fisher's combined probability test.

Quantitative PCR

Fresh whole pancreatic tissue was stored for at least 12 hours in RNA Later (Ambion) at -80C. RNA was extracted from whole tissue and sorted pancreatic cells using Trizol and RNeasy kit (Qiagen). Reverse transcription was performed using SuperScript III (Invitrogen). Expression of all genes was analyzed using Taqman assays (Applied Biosystems) and normalized to cyclophilin expression (Primers: GGCCGATGACGAGCCC, and TGTCTTTGGCTTTGTCTGCAA, probe: TGGGCCGCGTCTCCTTCGA)

Supplemental figure 1: Numb expression in the pancreas and during caerulein treatment

(*A*) Expression of Numb, but not Numb-like, is detected by qPCR in FACS isolated acinar cells. (*B*) Numb transcript expression in p48Cre and *p48Cre;Kras*^{G12D} whole pancreas upon caerulein treatment. The last day of caerulein treatment was designated as 'day 0'.

Supplemental Figure 2: Numb deletion does not significantly affect pancreatic development

(*A*) Numb deletion in *p48Cre;Numb*$^{f/f}$ mice as determined by qPCR on total pancreas RNA and (*B*) Western blot of total pancreatic lysate. Deletion of Numb does not affect normal pancreas development as indicated by (*C*) gross morphology, (*D*) H&E staining (*E*) immunostaining for E-cadherin (green), counterstained with DAPI (blue) and (*F*) immunostaining for Amylase (green) and CK19 (red), counterstained with DAPI (blue) in 6 week old, PBS treated animals. White arrows in F and F' point to CK19-positive ducts. (*G*) Ratio of β-cell (Insulin) to acinar cell (Cpa1) area and expression of pancreatic differentiation markers are not altered. (*H*) qPCR data of pancreatic differentiation markers expressed as mean ± SD. For qPCR analysis, N=3-4. Western blot image representative of N=3 per genotype.

Supplemental Figure 3: Tissue atrophy during pancreatic regeneration is due to Numb deletion in acinar cells

(*A, A'*) Gross morphology and (*B, B'*) immunostaining for YFP (green), Cpa1 (red) and DAPI (blue) and (*C, C'*) for YFP (green), CK19 (red) and DAPI (blue) on the same tissue section at 7 days after caerulein treatment in p48Cre^{ER};YFP and p48Cre^{ER};YFP;Numb$^{f/f}$ pancreata. Scale bars represent 100μm. (*D*) Pancreas mass:body weight ratio of PBS and caerulein treated mice at day 7. ** P<0.01, N=3.

Supplemental Figure 4: Enhanced and accelerated stromal and immune cell recruitment following caerulein treatment in *Numb* deleted mice

(*A,B*) Immunostaining for α-Smooth Muscle Actin (green) and CK19 (red) counterstained with DAPI (blue) at days 1 and 2 following caerulein treatment. (*C,D*). Immunostaining for CD45 (brown) counterstained with hematoxylin (blue) at days 1 and 2 following caerulein. Scale bars represent 100μm.

Supplemental Figure 5: Cells lacking Numb retain proliferative capacity

(*A-D*) Immunostaining for Ki67 (brown) counterstained with Alcian Blue. Scale bars represent 100μm.

Supplemental Figure 6: Caerulein-induced apoptosis of acinar cells in *p48Cre;Numb$^{f/f}$* mice is p53 independent

(*A,B*) Immunostaining for p53 protein (red) and E-cadherin (green), counterstained with DAPI (blue) 1-2 days after caerulein treatment in *p48Cre* and *p48Cre;Numb$^{f/f}$* mice. (*C*) Quantitative PCR analysis detects increased

expression of some pro-apoptotic genes, including p53 targets Noxa, Apaf1 and Puma as well as Bim. (*D*) No difference in pancreas size of *p48Cre;Numb$^{f/f}$* and *p48Cre;Numb$^{f/f}$;p53$^{f/f}$* pancreata at day 7 following caerulein treatment. (*E*) Pancreas mass to body weight ratio at day 7. Scale bars for (A-B) represent 50μm. qPCR data represented as individuals, overlaid with mean ± SD. * P<0.05.

Supplemental Figure 7: No gross differences are observed in *p48Cre^{ER};Kras^{G12D};YFP;Numb$^{f/f}$* pancreata compared to controls at postnatal day 2

Gross morphology (*A, A'*) and H&E (*B, B'*) images of p2 pancreata from *p48Cre^{ER};Kras^{G12D};YFP* and *p48Cre^{ER};Kras^{G12D};YFP;Numb$^{f/f}$* animals. Scale bars represent 100μm. (*C*) Pancreas mass:body weight ratio of PBS and caerulein treated mice at day 7.

Supplemental Table 1: Primary antibodies used for this study

Supplementary Figure 1

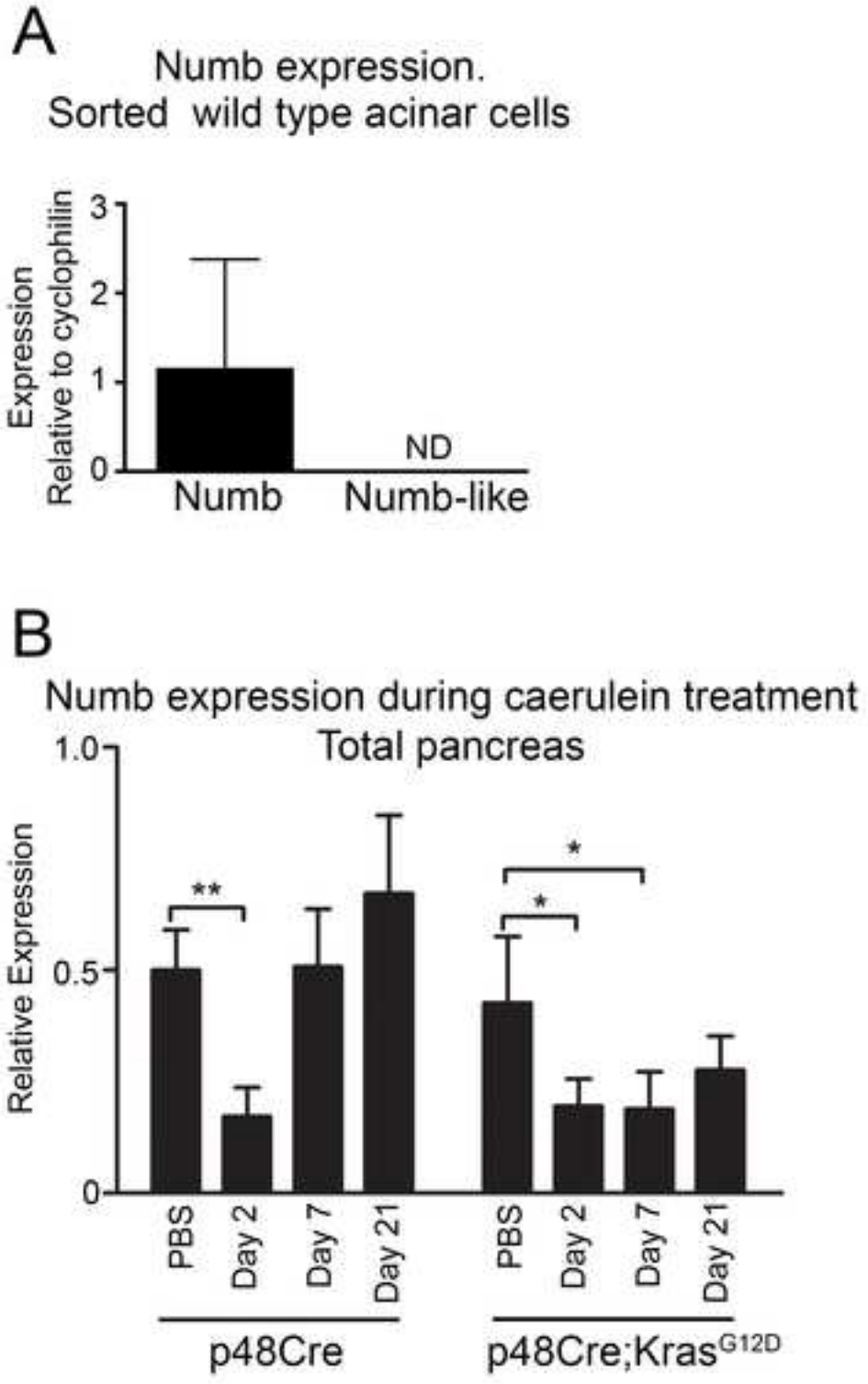

Supplementary Figure 2

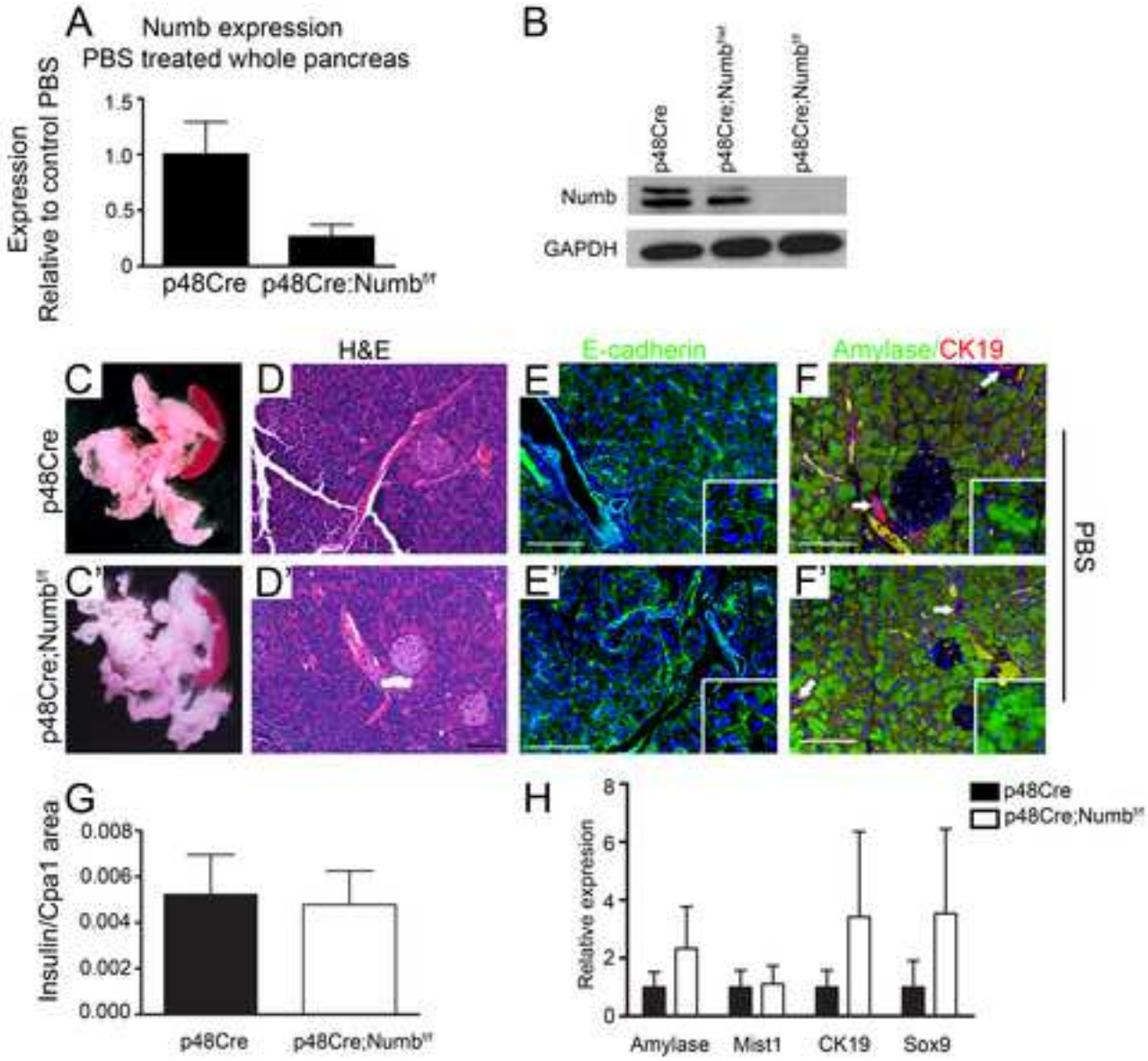

Supplementary Figure 3

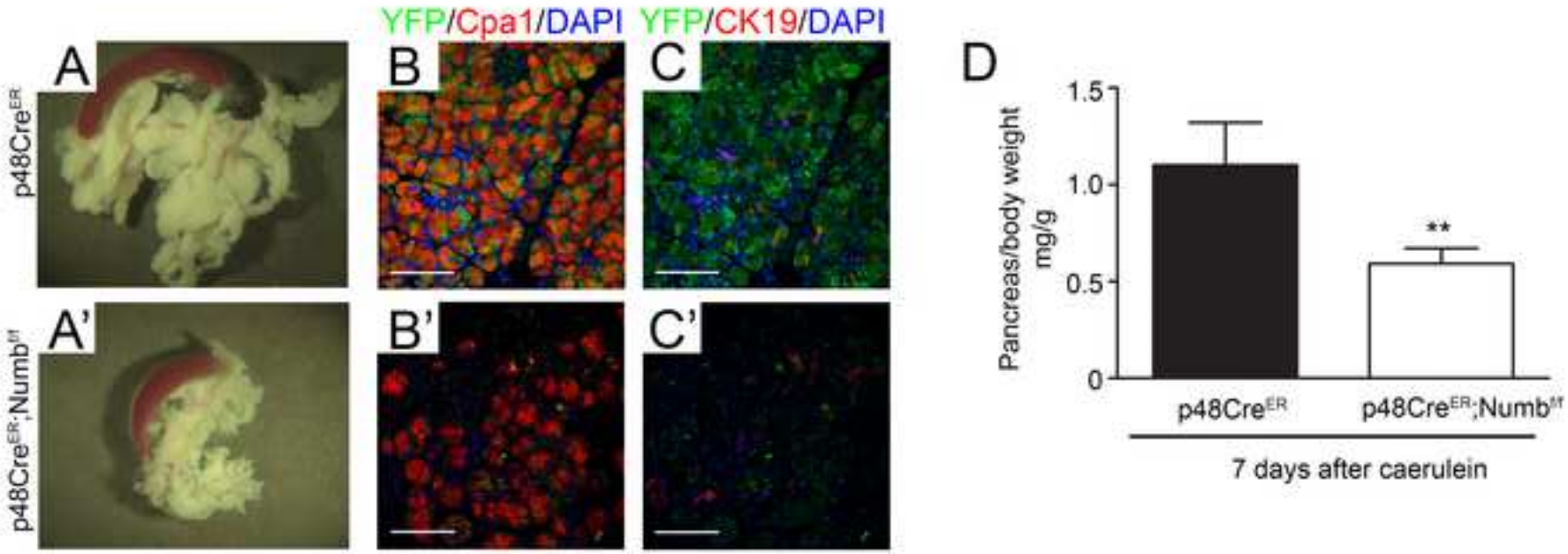

Supplementary Figure 4

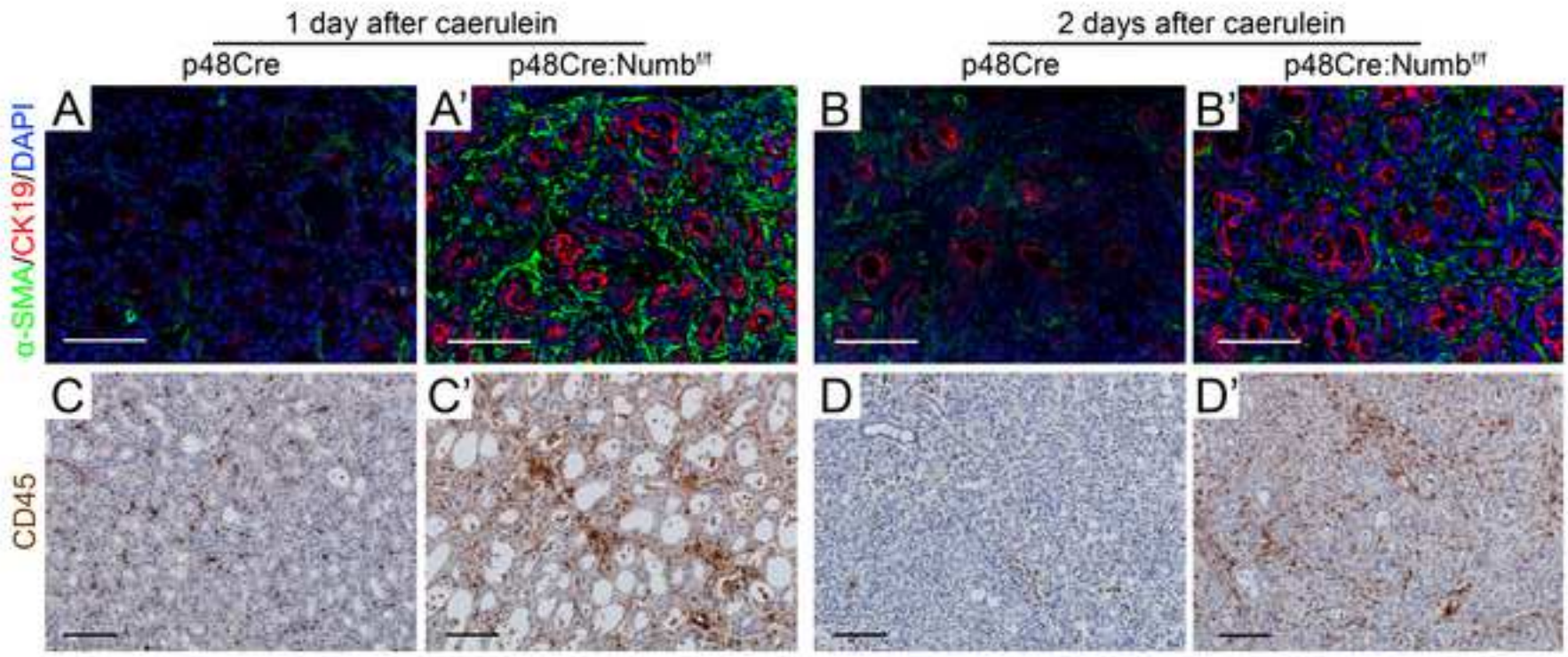

Supplementary Figure 5

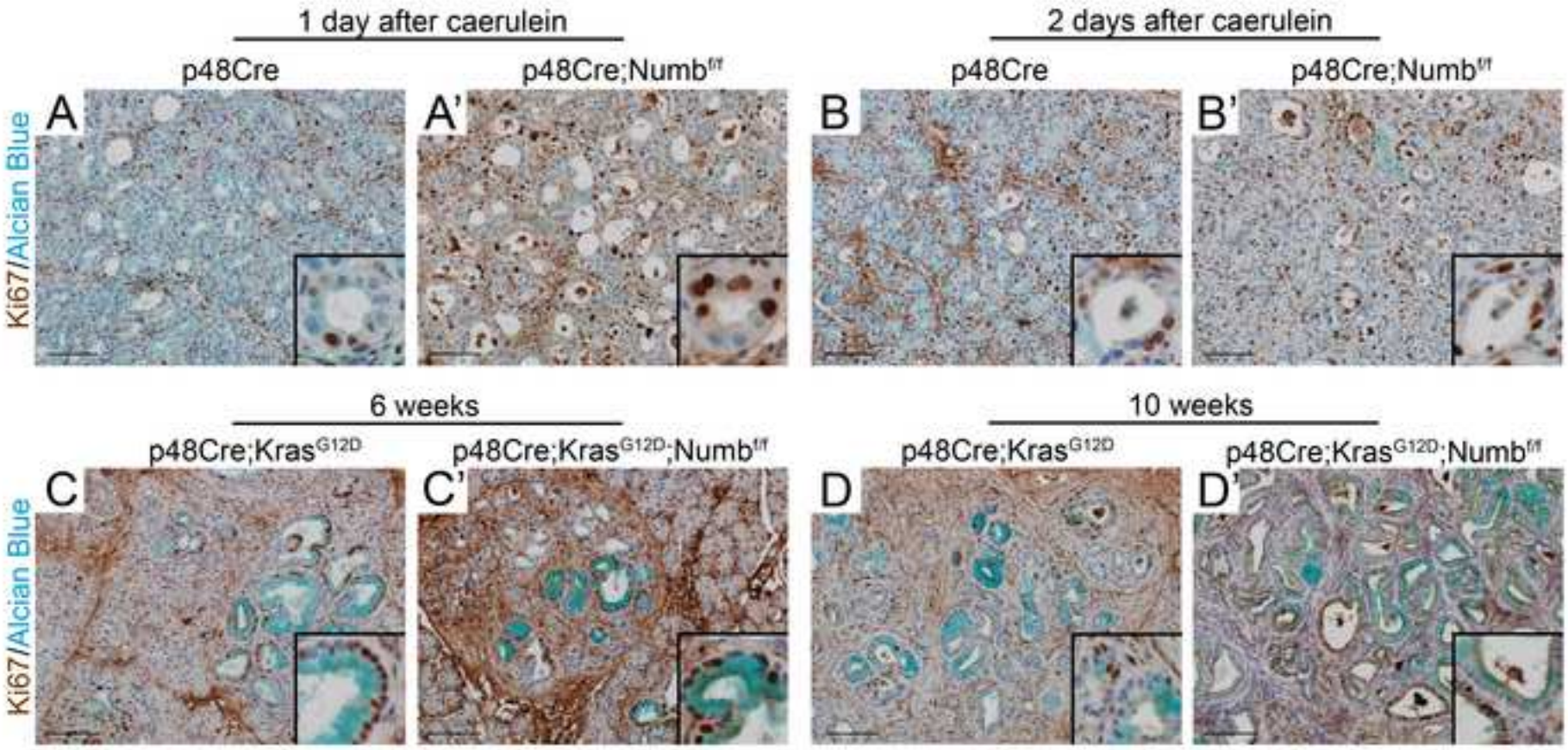

Supplementary Figure 6

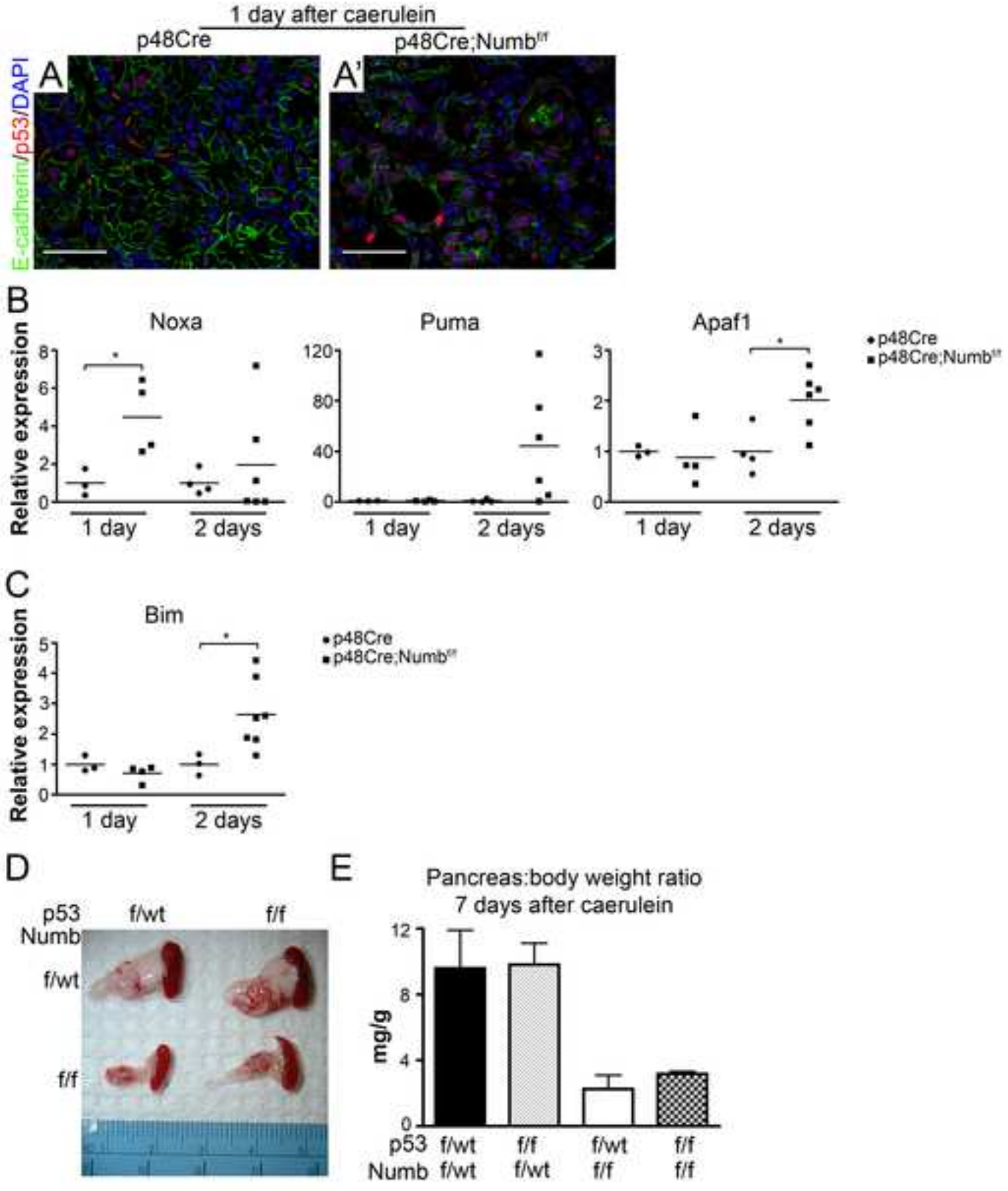

Supplementary Figure 7

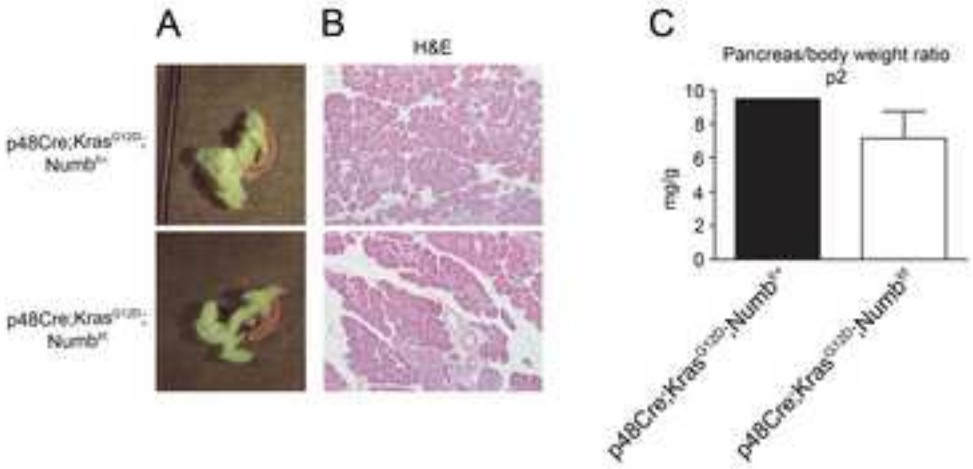

Supplementary Table 1

Antigen	Host Species	Source	Dilution	Application
α Smooth Muscle Actin	Mouse	Sigma-Aldrich	1:200	IF
Amylase	Rabbit	Sigma-Aldrich	1:200	IHC, IF
CD45	Rat	BD BioSciences	1:400	IHC
CK19 (TROMA III)	Rat	University of Iowa Hybridoma Bank	1:200	IF
CK19	Rabbit	Epitomics	1:400	IF
Cleaved Caspase 3	Rabbit	Cell Signaling Technologies	1:200	IF
Clusterin	Goat	Santa Cruz BioTechnologies	1:400	IF
Cpa1	Goat	R&D	1:200	IF
Phospho (Tyr576/577) FAK	Rabbit	Cell Signaling	1:1000	WB
GAPDH	Rabbit	Santa Cruz	1:10000	WB
GFP/YFP	Chicken	abcam	1:200	IF
Insulin	Guinea Pig	Linco	1:1000	IF
Ki67	Mouse	NovoCastra	1:200	IHC
Numb (Pan)	Rabbit	Chemicon	1:1000	WB
p53	Rabbit	Vector	1:400	IF

Supplemental Methods

Caerulein treatment

Acute pancreatitis was induced in p48Cre, p48Cre;Numb$^{f/f}$, p48Cre;Kras^{G12D} and p48Cre;Kras^{G12D};Numb$^{f/f}$ mice at 5-6 weeks after birth with a typical weight range of 22-25g by caerulein injection as previously described [13]. Briefly, mice received 8 hourly i.p caerulein injections (American Peptide Company), 2ug/injection on 2 consecutive days. Day 0 is counted as immediately following the final injection.

Immunohistochemistry and immunofluorescence

For histological, immunohistolochemical and immunofluorescence analysis, dissected pancreata were fixed with zinc buffered formalin (Anatech) overnight and embedded in paraffin wax. Heat mediated antigen retrieval was performed with Citra antigen retrieval solution (BioGenex) prior to staining. For immunofluorescence, AlexaFluor tagged secondary antibodies (1:400, Invitrogen) were used and slides were mounted using DAPI-containing Vectashield media (Vector). For Amylase, CK19 and CD45 immunohistochemistry, biotinylated goat anti-rat secondary (1:400, Vector) was used. 3-3'-Diaminobenzidine tetrahydrochloride was used as a chromagen. Sections were countedstained with Meyer's Hematoxylin and 1% Alcian Blue 8GX (Sigma) in 3% acetic acid solution where indicated. Primary antibodies used may be found in Supplementary Table 1.

Fluorescent images were acquired using Zeiss AxioImager and Leica SP5 confocal microscopes. Brightfield images were acquired using a Zeiss Axio Imager D1 microscope.

Western blotting

Primary antibodies are listed in Table S1. Secondary antibodies used were goat anti-rabbit IR800 and goat anti-mouse IR680 (1:15,000, LI-COR). Imaging was performed on a LI-COR Odyssey scanner and quantification was performed by normalizing fluorescence intensity of each individual band to the corresponding intensity of GAPDH.

Flow cytometry

FACS enrichment of acinar and ductal cells was performed as described by Morris et al (in preparation). Pancreata were digested with a series of reagents: 1) 2.5mg/ml Collagenase D (Roche) with 0.1ng/ml DNase I (Sigma-Aldrich) in Hank's buffered saline solution, 2) 0.05% Trypsin-EDTA, 3) 2U/ml Dispase (Invitrogen) in HBSS. Single cells were stained with FITC-conjugated anti-CD45 (1:400, eBioscience), PE-conjugated anti-CD49f (1:50, eBioscience) and Biotin-conjugated CD133 (Prominin1, 1:50, eBioscience). APC-conjugated streptavidin (1:100, eBioscience) was used as a secondary antibody. Cells were isolated using a FACS Aria (BD BioScience).

Quantification

For quantification of duct structures with luminal cells, percent metaplastic area and Alcian blue postive lesion count, 5-10 non-overlapping 100x (for p48Cre samples) or 200x (for $p48Cre^{ER}$;$Kras^{G12D}$ samples) H&E images were taken per

sample and scored by hand. Metaplastic area, in pixels, was selected by hand in Adobe Photoshop, Alcian blue positive lesions and duct structures with luminal cells were counted by hand and normalized to total area in pixels calculated by Metamorph. For Insulin/CPA1 area tissue sections from paraffin embedded pancreata were collected every 100μm through the entire organ. Sections were stained for Insulin and Cpa1 and total positive areas of each marker were calculated using a GE InCell Imager system.

Statistical Analysis

Results are shown as the mean ±SD. Paired data were evaluated using a two-tailed Student's *t*-test. Luminal cell count data was evaluated by Chi squared test. For meta-analysis of Numb expression in human PDA, 3 independent datasets[36-38] were utilized from the Oncomine microarray database (Compendia Bioscience, Ann Arbor, MI). Each study was evaluated independently using a two-tailed Student's *t*-test and a combined p value was calculated using Fisher's combined probability test.

Quantitative PCR

Fresh whole pancreatic tissue was stored for at least 12 hours in RNA Later (Ambion) at -80C. RNA was extracted from whole tissue and sorted pancreatic cells using Trizol and RNeasy kit (Qiagen). Reverse transcription was performed using SuperScript III (Invitrogen). Expression of all genes was analyzed using Taqman assays (Applied Biosystems) and normalized to cyclophilin expression (Primers: GGCCGATGACGAGCCC, and TGTCTTTGGCTTTGTCTGCAA, probe: TGGGCCGCGTCTCCTTCGA)

Supplemental figure 1: Numb expression in the pancreas and during caerulein treatment

(*A*) Expression of Numb, but not Numb-like, is detected by qPCR in FACS isolated acinar cells. (*B*) Numb transcript expression in p48Cre and *p48Cre;Kras*^{G12D} whole pancreas upon caerulein treatment. The last day of caerulein treatment was designated as 'day 0'.

Supplemental Figure 2: Numb deletion does not significantly affect pancreatic development

(*A*) Numb deletion in *p48Cre;Numb*$^{f/f}$ mice as determined by qPCR on total pancreas RNA and (*B*) Western blot of total pancreatic lysate. Deletion of Numb does not affect normal pancreas development as indicated by (*C*) gross morphology, (*D*) H&E staining (*E*) immunostaining for E-cadherin (green), counterstained with DAPI (blue) and (*F*) immunostaining for Amylase (green) and CK19 (red), counterstained with DAPI (blue) in 6 week old, PBS treated animals. White arrows in F and F' point to CK19-positive ducts. (*G*) Ratio of β-cell (Insulin) to acinar cell (Cpa1) area and expression of pancreatic differentiation markers are not altered. (*H*) qPCR data of pancreatic differentiation markers expressed as mean ± SD. For qPCR analysis, N=3-4. Western blot image representative of N=3 per genotype.

Supplemental Figure 3: Tissue atrophy during pancreatic regeneration is due to Numb deletion in acinar cells

(*A, A'*) Gross morphology and (*B, B'*) immunostaining for YFP (green), Cpa1 (red) and DAPI (blue) and (*C, C'*) for YFP (green), CK19 (red) and DAPI (blue) on the same tissue section at 7 days after caerulein treatment in p48Cre^{ER};YFP and p48Cre^{ER};YFP;Numb$^{f/f}$ pancreata. Scale bars represent 100μm. (*D*) Pancreas mass:body weight ratio of PBS and caerulein treated mice at day 7. ** P<0.01, N=3.

Supplemental Figure 4: Enhanced and accelerated stromal and immune cell recruitment following caerulein treatment in *Numb* deleted mice

(*A,B*) Immunostaining for α-Smooth Muscle Actin (green) and CK19 (red) counterstained with DAPI (blue) at days 1 and 2 following caerulein treatment. (*C,D*). Immunostaining for CD45 (brown) counterstained with hematoxylin (blue) at days 1 and 2 following caerulein. Scale bars represent 100μm.

Supplemental Figure 5: Cells lacking Numb retain proliferative capacity

(*A-D*) Immunostaining for Ki67 (brown) counterstained with Alcian Blue. Scale bars represent 100μm.

Supplemental Figure 6: Caerulein-induced apoptosis of acinar cells in *p48Cre;Numb$^{f/f}$* mice is p53 independent

(*A,B*) Immunostaining for p53 protein (red) and E-cadherin (green), counterstained with DAPI (blue) 1-2 days after caerulein treatment in *p48Cre* and *p48Cre;Numb$^{f/f}$* mice. (*C*) Quantitative PCR analysis detects increased

expression of some pro-apoptotic genes, including p53 targets Noxa, Apaf1 and Puma as well as Bim. (*D*) No difference in pancreas size of *p48Cre;Numb$^{f/f}$* and *p48Cre;Numb$^{f/f}$;p53$^{f/f}$* pancreata at day 7 following caerulein treatment. (*E*) Pancreas mass to body weight ratio at day 7. Scale bars for (A-B) represent 50μm. qPCR data represented as individuals, overlaid with mean ± SD. * P<0.05.

Supplemental Figure 7: No gross differences are observed in *p48Cre^{ER};Kras^{G12D};YFP;Numb$^{f/f}$* pancreata compared to controls at postnatal day 2

Gross morphology (*A, A'*) and H&E (*B, B'*) images of p2 pancreata from *p48Cre^{ER};Kras^{G12D};YFP* and *p48Cre^{ER};Kras^{G12D};YFP;Numb$^{f/f}$* animals. Scale bars represent 100μm. (*C*) Pancreas mass:body weight ratio of PBS and caerulein treated mice at day 7.

Supplemental Table 1: Primary antibodies used for this study